High Order, Reconstructor-Free Adaptive Optics for 6-8 meter class Telescopes

Maud Langlois[a,b], Roger Angel[a], Michael Lloyd-Hart[a], François Wildi[a], Gordon Love[b], Alexander Naumov[b]

[a]Steward Observatory, University of Arizona, Tucson, AZ 85721, USA
[b]University of Durham, Dept. of Physics, South Road, Durham DH1 3LE, United Kingdom

ABSTRACT

High order adaptive optics at high speed (1kHz), high accuracy (10 cm) and high photon efficiency requirements is needed for high contrast imaging in the infrared for exo-planet detection. An AO system with conventional deformable mirrors and reconstruction from slope measurements would be expensive and extremely difficult to produce. In this paper we describe a "reconstructor-free" high order adaptive optics system using a self-referenced Mach-Zehnder wavefront sensor and a liquid crystal phase corrector. Phase measurements are obtained directly from the two outputs the Mach-Zehnder interferometer, with $\pm\lambda/4$ pathlength difference between its two legs. The intensity difference between corresponding pixels on the two cameras outputs is proportional to phase error, provided this is small, and correction takes place at the pixel level with a liquid crystal phase corrector whose square geometry matches the wavefront sensor camera pixels. In this way high resolution and photon efficiency are achieved in a system with direct, pixel-based estimation, control and correction of phase error.

We have achieved in the laboratory wavefront retrieval with very fine scale sampling (128 phase measurements across the aperture) with $\lambda/30$ rms accuracy. Although the current electronics lacks dynamic range and speed, these could be readily improved for a real telescope system. Very recent progresses in decreasing the fall time of liquid crystal using the dual frequency method will allow for correction at kHz rates. While limited to correction of small wavefront amplitude errors (≤ 1 wave), such a system could be used very efficiently in tandem with a lower order system of high dynamic range.

1. INTRODUCTION

The adaptive optics systems currently operating or being made for the new generation of large optical telescopes are generally of low or moderate order, with actuator spacings projected to the entrance pupil of 0.5 m or larger. For some scientific goals higher order correction is both desirable and possible, because the targets are bright enough to allow very accurate wavefront measurement. One example is the search for faint brown dwarfs or planetary companions of nearby stars (Angel (1994a), Stahl and Sandler (1995)) that requires very high contrast ratio very close to the star. In particular, accurate fine spatial scale wavefront correction in the near infrared would allow for ground-based direct detection of exo-planets when associated with interfero-coronography techniques (Langlois *et al.* (2001)).

Adaptive optics systems with wavefront correction on a scale of $\sim$12 cm has been achieved on smaller telescopes, such as SOR 3.5 m (Spinhirne *et al.* (1998)) and Mt Wilson 2.5 m (Shelton *et al.* (1995)), to produce diffraction limited images at optical wavelengths. In this paper we consider wavefront correction on this fine scale for 6-8 m class telescopes, which will require some 3000 actuators. We emphasise on the reconstructor free phase measurement and evaluate both theoretical and experimental efficiencies.

Further author information: (Send correspondence to M. P. Langlois)
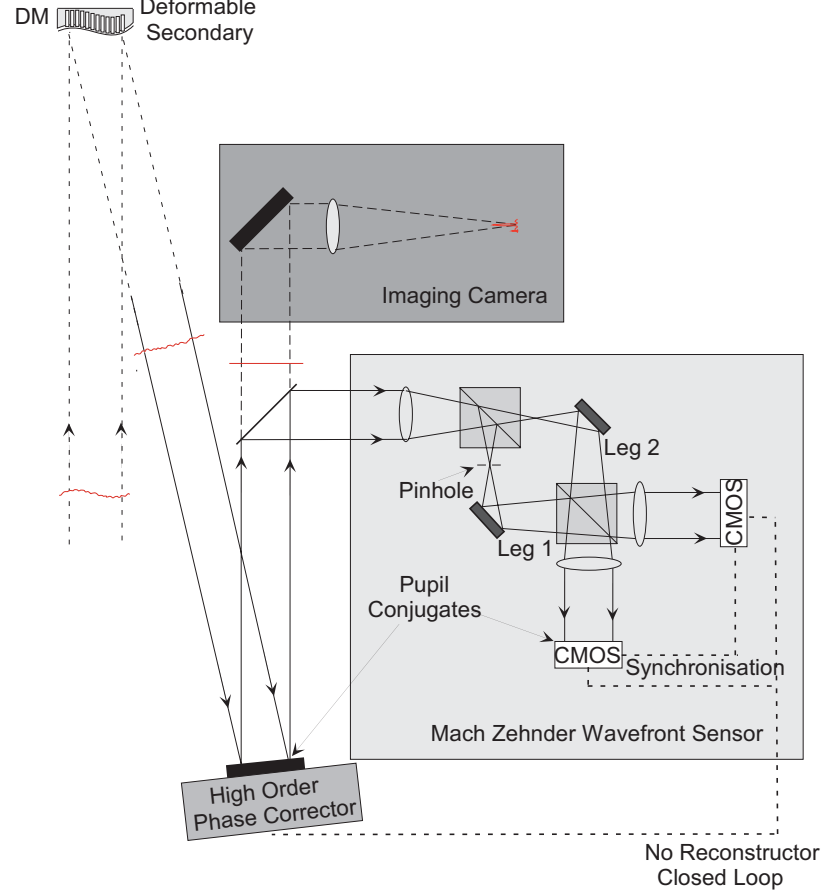M. P. Langlois : E-mail: maud.langlois@durham.ac.uk

Figure 1. High order AO system: *The Mach-Zehnder senses the residual phase variation downstream of the low order secondary deformable correction. In one of its arms, a pinhole filters the wavefront to produce a reference beam. After recombination two pupil images are formed on two detectors. Their intensity difference directly measures the phase that is sent to adjust the corresponding deformable mirror actuator or phase modulator pixel.*

2. PRINCIPLE

We consider the case of dual stage wavefront correction, where low order, high amplitude wavefront errors are corrected by a first stage adaptive optics system, for example the deformable secondary system for the 6.5 m MMT, Lloyd-Hart *et al.* 2000. The errors left uncorrected after that first stage of correction are estimated by a Mach-Zehnder self referenced wavefront sensor and corrected by a complementary pixelized corrector such as a liquid crystal phase modulator (Gourlay *et al.* (1997)) or a different corrector with a high number of actuators on a square geometry (Zamkotsian *et al.* (1999), Langlois *et al.* (1999)).

The goal to be achieved by the wavefront sensor is to measure the phase errors with very high accuracy at small spatial scales. The residual phase error under normal seeing conditions at the MMT should be around 300 nm rms after the deformable secondary correction. In order to achieve the high Strehl (85-98 %) required to detect exo-planets, wavefront measurement with 0.4-0.1 rms radians ($\frac{\lambda}{13}$- $\frac{\lambda}{4}$ P-V) accuracy on 5-10 cm spatial scale must be achieved by the Mach-Zehnder sensor. The temporal scale of the correction is very short for high order AO. The update rate is around 1-2 Khz (Madec *et al.* (1992)), assuming 2000 Zernike modes of correction, a wind velocity of 20 ms^{-1} and that the cutoff open loop frequency is 20 times smaller than the update rate in order to meet the high efficiency required for very faint companions detection.

The principle is to measure the residual wavefront errors directly by using the two outputs of a Mach-Zehnder interferometer (Angel (1994a)), as shown on Figure 1. In one arm of the interferometer, a pinhole acts as a spatial filter to provide the spherical reference wavefront. After recombination at the output beamsplitter, two images of the pupil are formed on two imaging detectors (CMOS). When the optical pathlength difference between the two legs is $\frac{\lambda}{4}$ the two images are equal in intensity, resulting in a null difference image. A small local phase difference between the two legs results in the difference signal at that location being equal to the phase for small phase differences. In consequence the difference in intensity between corresponding pixels on

the two cameras (CMOS 1 & 2) gives directly the phase at that pixel location on the pupil. This is equivalent to a two-steps retrieval algorithm.

3. THEORETICAL PERFORMANCES AND LIMITATIONS

The total measurement error (σ^2_{total}) can be separated into phase retrieval error (σ^2_{ret}) that is related to the limited dynamic range of the measurements, reference error (σ^2_{ref}), photon and detector noise (σ^2_{photon}), wavefront fitting ($\sigma^2_{fitting}$), and temporal wavefront error ($\sigma^2_{temporal}$), as given by

$$\sigma^2_{total} = \sigma^2_{ret} + \sigma^2_{photon} + \sigma^2_{ref} + \sigma^2_{fitting} + \sigma^2_{temporal} \tag{1}$$

The three first contributions to the total variance, σ^2_{total} are related to the spatial filtering. σ^2_{ref} is the residual wavefront variance after spatial filtering, σ^2_{ret}, and σ^2_{photon} are related through the fringe visibility to the intensity variation of the filtered beam. When the loop is closed, σ^2_{ret} and σ^2_{ref} become negligible compared to the other error contributions. Rather the fundamental limits to the correction quality is set by noise, fitting and temporal errors. They ultimately define the sensitivity of any type of wavefront sensor.

The fitting error is given by Hudgin (1977)

$$\sigma^2_{fitting} = 0.4(\frac{\Delta x}{r_0})^{\frac{5}{3}}, \tag{2}$$

where r_0 is the coherence length of the turbulence. This expression that represents optimum reconstruction from discrete phase measurements over a square pixel of dimension Δx assuming turbulence frozen on a moving layer. The temporal error is given by:

$$\sigma^2_{temporal} = (\frac{w\Delta t}{r_0})^{\frac{5}{3}}, \tag{3}$$

where w is the effective speed relating spatial end temporal errors ($w = 3.2V_{wind}$).

The wavefront measurement obtained by the Mach-Zehnder is estimated against the reference wavefront spatially filtered by a pinhole. Both the quality of that reference wavefront and the amount of light passing through the pinhole depends on its size. While the quality of the reference light beam directly affects the accuracy of the phase measurement, the amount of light affects the signal to noise of the fringes and in consequence the measurement accuracy. Appropriate pinhole sizes for the MMT high order AO system range from 1.2 to the diffraction limited FWHM (Langlois *et al.* 2002). The optimum wavefront measurement is achieved for the smallest pinhole that equilibrates photon noise error attributed to visibility and intensity fluctuations and, the reference wavefront error.

Wavefront measurement error is also introduced when retrieving the phase information by both photon and detector noises. Langlois (2001b) showed that this error is given by:

$$\sigma^2_{photon} = \frac{1 + 2(\frac{R}{QeN(x)})^2}{N(x)V(x)^2}, \tag{4}$$

where N(x) is the total number of photon per pixel available for the interferometer, V(x) is the visibility of the interferogram, R is the detector readout noise and Qe the quantum efficiency. Note that σ^2_{photon} expressed by (4) is comparable to σ^2_{photon} for negligible readout, as given in Angel (1994a) and Angel *et al.* (1994b) when a three-steps retrieval algorithm is used. Assuming a spatial filter 1.6 FWHM in diameter, the visibility varies by a factor of 1.15 from the center of the pupil to the edge. If needed, it is still possible to eliminate this effect by calibrating out the visibility function for various pinhole settings. In that case, the photon and detector noise gives a phase accuracy of 0.15 rms accuracy for stars brighter than $m_R = 7$ for $R = 5e^-$ and, $m_R = 5.5$ for $40e^-$ detector readout that represents the level achieved with respectively the CCD and CMOS detector technology. This estimation represents the optimum accuracy achievable by the MMT for high order correction when correcting at 5 cm spatial scale. If using a larger collecting area like the Large Binocular Telescope (2x8.4m) the same accuracy will be obtained for star magnitudes 1.0 to 1.5 fainter.

In the case of the MMT the expected total residual variance, as presented in Figure 2 shows two distinct regions according to the amount of light available. When the target star is bright the photon noise, σ^2_{photon}, is negligible compared to the other contributions. For guide stars fainter than 7th magnitude the photon error predominates and the total residual wavefront error, σ^2_{total}, is independent of the atmospheric conditions. For
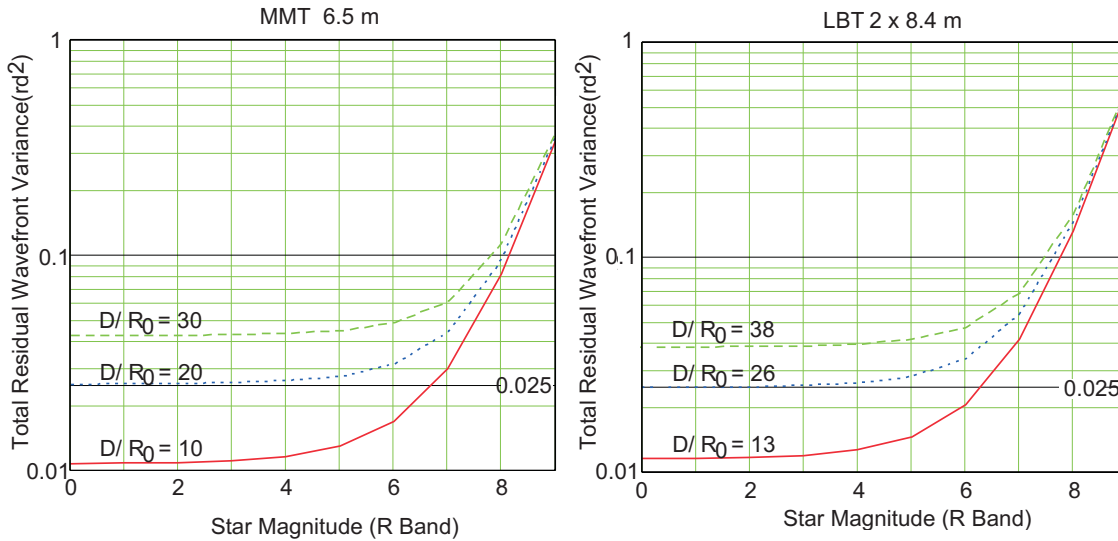
Figure 2. *Total wavefront variance as estimated from equation (1).* **Left:** *For the MMT high order system correcting at 5 cm spatial scale as a function of the R band star magnitude and for several seeing strengths. The parameter values are $R = 5$ e^- and the integration time $t = 0.5$ ms.* **Right:** *For the LBT high order AO system correcting at 3.3 cm spatial scale and for the same seeing conditions and parameter values.*

128 pixels across the pupil corresponding to 5 cm correction scale, 96% Strehl ratio is obtained for average seeing and for star brighter than $m_R = 7$; for stars six times fainter it drops to 70%.

The dynamic range of the phase measurements is limited by the retrieval algorithm. The wavefront can only be estimated without ambiguity if the phase difference between neighboring pixels is smaller than $\pm\lambda/4$ for the two steps retrieval algorithm. When the turbulence is stronger than $\frac{D}{r_0} > 20$ the amplitude of the phase to be measured can exceed the non ambiguity range. In that case, a more robust retrieval algorithm should be used, such as two-plus-one or a three-steps algorithm with $\frac{\pi}{2}$ shift between the interferograms where 0.001-0.005 rd^2 accuracy can be achieved under strong turbulence conditions (Colucci 93). If using one of these more elaborated phase retrieval algorithms the limitation in phase amplitude is twice as much as for the two interferograms algorithm and the non ambiguity criterion will be satisfied for $\frac{D}{r_0} < 40$. The three-steps reconstruction phase shifting algorithm can be easily implemented by using a fast response piezo-electric translation stage to drive the non filtered Mach-Zehnder Interferometer leg mirror where a 0 and a $-\frac{\pi}{2}$ steps would produce the three interferograms needed on the two detector in two steps t_1 and t_2. The phase would be then reconstructed without visibility dependency. Conceding half the integration time with the three-steps would allows to improve by a factor two the dynamic range of the Mach-Zehnder interferometer and extend its range of correction to shorter wavelength or more drastic seeing condition. But the present design matches the requirements for the MMT high order AO system, measuring wavefront errors at 0.8 μm to better than 0.01 rd^2 for 0.4 arc-seconds seeing condition and 0.1 rd^2 for 0.55 arc-seconds seeing.

Chromatic effects and intensity difference between the two beams also affect the contrast of the fringes. The intensity difference between the two beams can be properly compensated by using a passive interchangeable or active intensity modulator. The bandwidth of the wavefront measurement is set by the coherence length, $L_{coh} = \frac{\lambda^2}{2\Delta\lambda}$, where λ is the central wavelength and $\Delta\lambda$ is the full spectral bandwidth. The bandwidth increases with the observing wavelength and decreases with phase errors to be estimated. In our case the wavefront peak-to-valley error is smaller than $\lambda/2$ P-V, and the maximum bandwidth is equal to the wavelength of operation. Such criterion sets a rather large bandwidth and in fact, the bandwidth of the system will be 2 times smaller if using a liquid crystal phase modulator to correct the phase errors as set by the dispersion of its birefringence.

The size of the pupil on the detector is an important issue, there is a trade-off between using as many pixels across the pupil diameter to minimize the wavefront fitting error and using as few pixels as possible to increase the signal per pixel and to improve the sensibility. A major advantage for a wavefront sensor is its flexibility to adjust the pupil sampling with the target brightness in real time, being easily achieved with the Mach-Zehnder wavefront sensor by binning detectors pixels.

4. CLOSED LOOP OPERATION

In order to take advantage of the direct phase estimation at pixel level the correcting device, a phase corrector with a square geometry corresponding to the detector geometry is required. In closed loop operation both corrector and detectors components will communicate via a simple digital signal differentiation electronics without involving a reconstructor as shown in Figure 3.

We investigated various correctors for the high order AO system, the liquid crystal phase modulator were the more readily available and we were able to use a 128x128 pixels one[*] for our experiment. These types of correctors have traditionally limited response time specially for large amplitude of correction. Recently, some progress has been made in decreasing the fall time of liquid crystal. Presently, fast response liquid crystals relying on dual frequency material (Restaino *et al.* 00) have demonstrated switching speeds around 120 μs for $\pi/4$ phase switching. Also recent progresses have been achieved to improve the liquid crystal throughput to 65% and 80% fill factor. These improvements pave the way toward high order liquid crystal correction at the telescope, the remaining limitation being the bandwidth of the correction. The bandwidth of a liquid crystal corrector is set by the dispersion of its birefringence relative to the dispersion of air. In this particular case the residual errors are smaller than $\lambda/10$ P-V at the edges of the 0.7 μm and 0.35 μm bandwidth for a central wavelength at 1.0 μm and 0.7 μm respectively. These devices can be made polarization independent by adding a quarter wave plate, as proposed by Love (1993) and Kelly *et al.* (1999). In such case polarization independent phase modulation was obtained over 0.200 μm wavelength band with Strehl ratio greater than 90% by using an zero order quarter wave plate between the active liquid crystal pad and the reflective surface.

Practical wavefront sensors for stellar wavefront measurements require fast read out, low noise, and high quantum efficiency detectors. Although the CMOS detectors are not yet optimized for these two latest requirements, they offer a fundamental advantage for the experiment, where their pixels are addressed and read out directly, so the phase information they contain may be directly sent to the corresponding corrector pixel. In consequence there is no delay between reading of a pixel's charge and its output electrical signal, avoiding the delay while charge is transferred out of regular CCD and the numerical processing can be done in parallel. In addition, CMOS devices are characterized by the absence of shutter, that contribute to minimize the latency period. Speedwise, the CMOS technology at the present time is capable of offering 1kHz frame rate for a 512x512 pixel format. The drawback with these detectors is the 40 e$^-$ readout and the 25% quantum efficiency.

The real time control electronics to close the loop is simple and emphasis on pixel by pixel processing without delay time. The electronic control is divided in three stages as shown on Figure 3:

- Synchronization of the two cameras is done using a common external clock and by producing a simultaneous starting reference for the two devices,

- Phase recovery is performed on a pixel-to-pixel based subtraction of the two Mach-Zehnder output images,

- Interface with the corrector includes an integrator to stabilized the loop.

5. EXPERIMENTAL PERFORMANCES

A laboratory demonstration was conducted in order to test the Mach-Zehnder concept for closed loop operation. The setup depicted on Figure 3 is reduced to its basics: a Mach-Zehnder interferometer, a liquid crystal spatial phase modulator (LC), a set of electronics to retrieve the phase, and a laser diode operating at 635 nm with few millimiters coherence length for the light source. Such experiment allowed a direct measurement of small local phase variation, generated by the spatial phase modulator.

We used two identical CMOS detectors[†] with on chip programmable capability, and frame rate ranging from 50 to 100Hz. The detectors registers are programmed to produced a 128x128 output image matching the liquid crystal phase modulator format. Exact matching of corrector and camera pixels size and position is an issue that ultimately affects the wavefront correction accuracy and is crucial for the success of the closed loop. Each detector needs to be aligned very accurately with respect to the second detector and to the wavefront corrector and the magnification between each components needs to be carefully matched. The two cameras were aligned with each other within $\pm$ 0.3 pixel error in translation, 0.1 degree in rotation (1/5 pixel) and 0.99% in magnification corresponding to 1.3 pixels across the full aperture. The alignment parameters errors set the

---

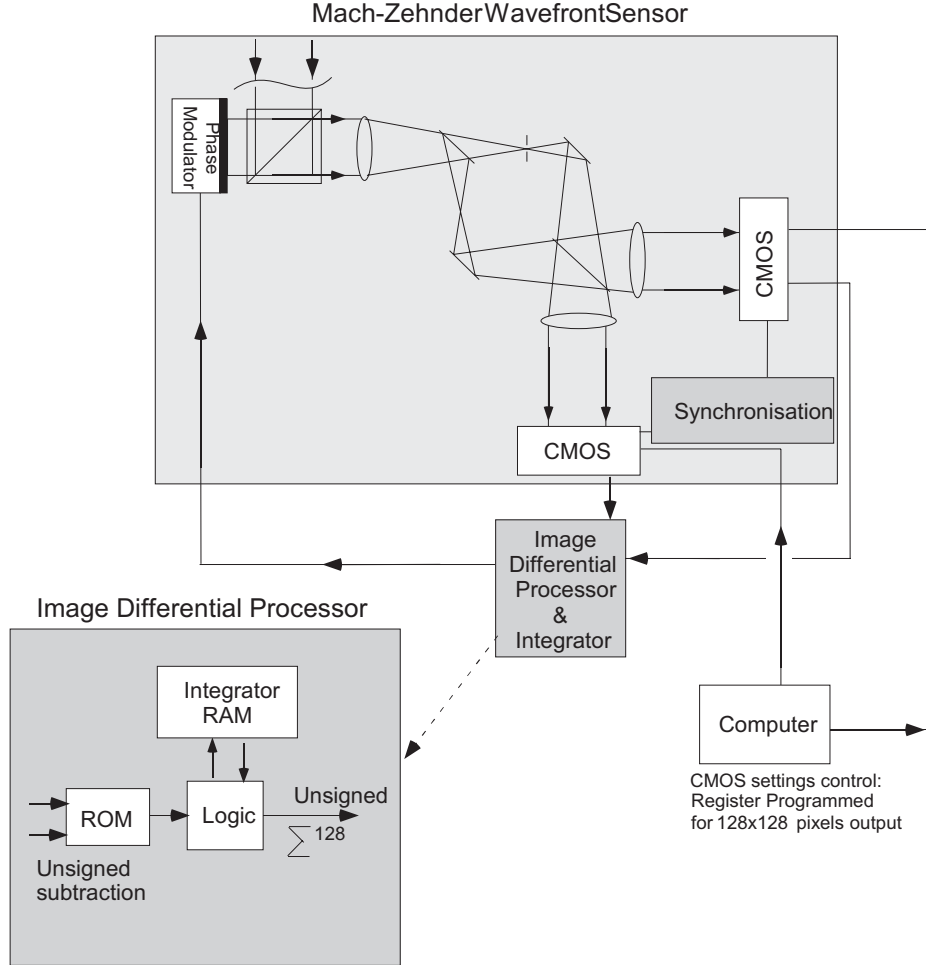[*]from Boulder Non Linear Systems
[†]from Photobit

Figure 3. *The scheme for the real time control electronics closing the loop on the SLM by using the Mach-Zehnder phase measurement recorded on two CMOS detectors.*

limits on the resolution that can be achieved with such WFS. They were found to be smaller than a third of a pixel and they could be reduced to within a fifth to a tenth of a pixel where the manufacturing errors stand. The pixel size manufacturing errors, which is estimated to be between 6 and 10% of the detector length and only 0.25% of the pixel length for the liquid crystal is another important consideration. Because of mismatches between the detector and liquid crystal pixel geometry from manufacturing errors, a Moiré pattern appears.

Practically we were able to estimate the phase sensitivity of the Mach-Zehnder WFS by producing a 2 levels of phase input image as shown on Figure 4C.2 with small phase difference between the two ($\lambda/18$). The image corresponding to the phase measurement (Figure 4C.1), where the difference of the two outputs response is recorded has an average visibility equal to 0.3, due to the fact that the beam intensity of the two legs could not be equilibrated properly without introducing too many aberrations but also to the slight difference in polarization between the two legs. The visibility varies by a factor 1.3 between the pupil center and the edge, resulting from spatial filtering by the 1.5 FWHM diameter pinhole. The slight misalignment between the two cameras causes a small blurring. The main limitation for estimating the phase came from the non-uniform Moiré pattern caused by the pixel geometry matching discrepancy between the cameras and the liquid crystal corrector, due to the low quality of the detectors. It can ultimately be corrected by tighter requirements for the camera pixel geometry. Such effect is clearly seen on the Figure 4C.1 were it overlaps with a small amount of phase aberration between the two legs of the interferometer. Both the Moiré pattern and phase aberration background contributions can be removed to produce an uniform background across the 5 mm aperture by using more precise components. we removed the non uniform background from the initial image by numerical post processing . The result of this background subtraction, as shown on Figure 4C.3, matches very closely the input image loaded on the liquid crystal phase modulator. The residual phase error given by the difference between the input phase and the measurement is smaller by a factor 5 times the $\lambda/18$ initial phase difference. Most of the residual error comes from the edges of the writing and are caused by lack of resolution when imaging liquid crystal pixels on the cameras.
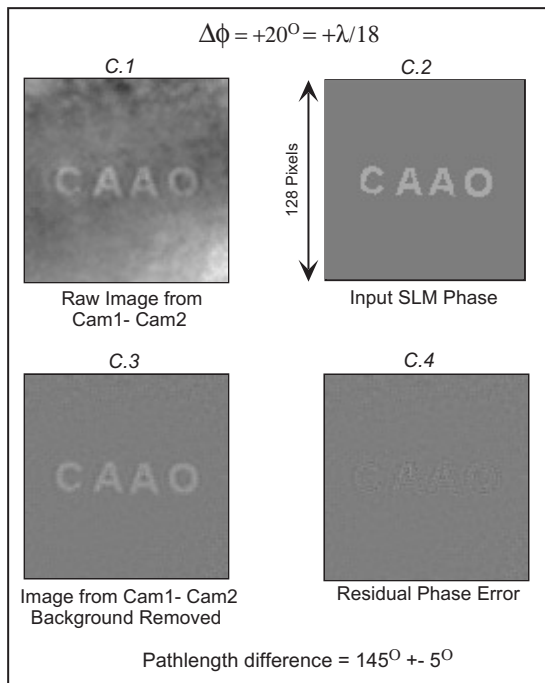
Figure 4. *The $\lambda/18$ Phase Measurement obtained with both camera. The two levels of phase input image with known phase difference between the two levels (C.2) is downloaded on the SLM. The corresponding difference camera image (C.1) is the measurement of the phase by the Mach-Zehnder. The same image with the background subtracted (C.3) is very similar to the phase image generated by the SLM (C.2). The residual measurement phase error (C.4) is the difference between the two (C.3 - C.2).*

6. CONCLUSIONS

High resolution wavefront measurements involving no reconstructor neither computer numerical processing is achievable with the current technology and we have demonstrated the feasibility principle with 128x128 degrees of correction. Both the phase sensitivity and accuracy achieved were extremely good. At the telescope similar results can be achieved if the detectors are upgraded for faster ones, such as the existing ones that run at more than 2.2kHz (Allan *et al.*(2001), Bloss *et al.*(2000)), leading to 90% Strehl ratio in R band when using a very bright guide star. In order to achieve the ultimate planet detection goal readout noise and quantum efficiency would need to be improved to levels achieved with EEV CCD detectors, i.e. 1-3 e^- and 40% QE. While improvements in readout noise would reduce the wavefront measurement error, QE improvements would increase the magnitude range for the guiding targets. In fact more light efficient detectors such as CCDs could also be used at a small time latency cost and we could envision re-imaging the two pupil on a single detector.

The new Mach-Zehnder wavefront sensor has the capability of measuring the wavefront on very small scales with extremely high accuracy without a reconstructor. As a result it opens the path to very high order wavefront measurement and correction and a new era for observational astronomy by offering both resolution improvement and scattered light minimization. One of the application that would highly benefits from these improvements is the search for extremely faint star companions such as extra-solar planets.

REFERENCES

J. R. P. Angel, "Ground-based imaging of extrasolar planets using adaptive optics", *Nature* **368**, 203, 1994a.

S. M. Stahl, and D. G. Sandler, "Optimization and performance of adaptive optics for imaging extrasolar planets", *APJ Letters* **454:L153**, 1995

M. Langlois, J. R. P. Angel, and P. Hinz, "Detection of extra-solar planets with large ground based telescopes", to be submitted to *PASP*, 2001.

J. M. Spinhirne, J. G. Allen, G. A. Ameer, J. M. B. II, J. C. Christou, T. S. Duncan, R. J. Eager, M. A. Ealey, B. L. Ellerbroek, R. Q. Fugate, G. M. Jones, R. M. Kuhns, D. J. Lee, W. H. Lowrey, M. D. Oliker, R. E. Ruane, D. W. Swindle, J. K. Voas, W. J. Wild, K. Wilson, and J. L. Wyania, "The starfire optical range 3.5m telescope adaptive optical system", in *Adaptive Optical System Technologies*, D. Bonaccini and R. K. Tyson, eds., *Proc. SPIE* **3353**, 22, 1998.

C. Shelton, T. Schneider, D. McKenna, and S. Baliunas, "First tests of the cassegrain adaptive optics system of the mount wilson 100-inch telescope", in *Adaptive Optical Systems and Applications*, D. Bonaccini and R. K. Tyson, eds., *Proc. SPIE* **2532**, 72, 1995.

M. Lloyd-Hart, F. P. Wildi, B. Martin, P. C. McGuire, M. A. Kenworthy, R. L. Johnson, B. C. Fitz-Patrick, G. Z. Angeli, S. M. Miller, and J. R. P. Angel, "Adaptive Optics for the 6.5-m MMT", in *Adaptive Optical Systems Technology*, P. L. Wizinowich Ed., *Proc. SPIE* **4007**, 167, 2000.

J. Gourlay, G. D. Love, P. M. Birch, R. M. Sharples, and A. Purvis, "A real-time closed-loop liquid crystal adaptive optics system: first results", *Optics Communications* **137**, 17, 1997.

F. Zamkotsian, and K. Dohlen, "Surface characterization of micro-optical components by Foucault's knife-edge method: the case of a micromirror array", *Applied Optics* **38**, 6532, 1999.

M. P. Langlois, J. R. P. Angel, M. Lloyd-Hart, S. M. Miller, and G. Z. Angeli, "High-order adaptive optics system with a high-density spherical membrane deformable mirror", in *Adaptive Optics Systems and Technology*, Robert K. Tyson and Robert Q. Fugate Eds., *Proc. SPIE* **3762**, 50, 1999.

P.-Y. Madec, J.-M. Conan, and G. Rousset, "Temporal characterisation of atmospheric wavefront for adaptive optics", in *Progress in Telescope and Instrumentation Technologies*, Marie-Helene Ulrich Ed., *ESO Proc.* **42**, 471, 1992.

R. J. Hudgin, "Wavefront compensation error due to finite corrector-element size", *J. Opt. Soc. Am.* **67**, 393, 1977.

M. Langlois, J. R. P. Angel, M. Lloyd-Hart, and F. Wildi, "Very high order reconstructor free adaptive optics", to be submitted to *PASP*, 2002.

J. R. P. Angel, "Optimization of wavefront sensor for the highest accuracy and sensitivity", in *Adaptive Optics for Astronomy*, D.M. Alloin and J.-M. Mariotti Eds., *Proceedings of the NATO Advanced Study Institute* **423**, 139, 1994b.

D. Colucci, "Atmospheric wavefront sensing and correction including the stellar phase interferometer", *PhD thesis*, University of Arizona, 1993.

M. P. Langlois, "High order adaptive optics to detect faint companions around nearby stars", *Phd Thesis*, University of Paris 7, 2001b.

S. R. Restaino, J. T. Baker, D. C. Dayton, and L. G. Finkner, "Experimental results from an adaptive optics system based on a dual frequency nematic device,", in *Liquid Crystal Materials, Devices, and Flat Panel Displays*, Ranganathan Shashidhar and Bruce Gnade Eds., *Proc. SPIE* **3955**, p. 54, mar. 2000.

G. D. Love, "Liquid crystal phase modulator for unpolarized light", *Appl. Opt.* **32**, 2222, 1993.

T.-L. Kelly and G. D. Love, "White light performance of a polarization independent liquid crystal phase modulator", *Appl. Opt.* **38**, 1986, 1999.

G. R. Allan, D. Dattani, D. R. Dykaar, E. C. Fox, S. G. Ingram, S. R. Kamasz, M. J. Kiik, B. Li, A. Pavlov, Q. Tang, "High-speed VGA CMOS image sensor", in *Sensors and Camera Systems for Scientific, Industrial, and Digital Photography Applications*, Morley M. Blouke, John Canosa, and Nitin Sampat Eds., *Proc. SPIE* **4306**, 111, 2001.

H. S. Bloss, J. D. Ernst, H. Firla, S. C. Schmoelz, S. K. Gick, and S. Lauxtermann, "High-speed camera based on a CMOS active pixel sensor", in *High-Speed Imaging and Sequence Analysis*, Alan M. Frank and James S. Walton Eds., *Proc. SPIE* **3968**, 31, 2000.